

Discussing the Relationship between the Static and Dynamic Light Scattering

Yong Sun

November 8, 2018

Abstract

Both the static (*SLS*) and dynamic (*DLS*) light scattering techniques are used to obtain the size information from the scattered intensity, but the static radius R_s and the apparent hydrodynamic radius $R_{h,app}$ are different. In this paper, the relationship between SLS and DLS is discussed using dilute water dispersions of two different homogenous spherical particles, polystyrene latexes and poly(*N*-isopropylacrylamide) microgels, with a simple assumption that the hydrodynamic radius R_h is in proportion to the static radius R_s , when Rayleigh-Gans-Debye approximation is valid. With the assistance of the simulated data, the apparent hydrodynamic radius $R_{h,app}$ has been discussed. The results show that the apparent hydrodynamic radius is different with the mean hydrodynamic radius of particles and is a composite size obtained from averaging the term $\exp(-q^2 D\tau)$ in the static size distribution $G(R_s)$ with the weight $R_s^6 P(q, R_s)$.

It is known that the structural information and mass weight are included in the relationship between the average scattered intensity and the scattering angle. Measuring this dependence is called the static light scattering (*SLS*). The analysis of the time auto-correlation of the scattered light intensity can provide the dynamic information of particles, called the dynamic light scattering (*DLS*). SLS obtains the information from the optical features and DLS gets the information from both the optical and hydrodynamic characteristics of particles. If the relationship between the optical and hydrodynamic quantities of particles can be built, the experimental values of the normalized time auto-correlation function of the scattered light intensity $g^{(2)}(\tau)$ can be expected using the size information obtained from SLS. In this article, the relationship between the SLS and DLS for homogenous spherical particles is discussed with a simple assumption when Rayleigh-Gans-Debye (*RGD*) approximation is valid.

For homogeneous spherical particles where the RGD approximation is valid, the normalized time auto-correlation function of the electric field of the scattered light $g^{(1)}(\tau)$ is given by

$$g^{(1)}(\tau) = \frac{\int_0^\infty R_s^6 P(q, R_s) G(R_s) \exp(-q^2 D\tau) dR_s}{\int_0^\infty R_s^6 P(q, R_s) G(R_s) dR_s}, \quad (1)$$

where q is the scattering vector, R_s is the static radius, τ is the delay time, D is the diffusion coefficient, $G(R_s)$ is the number distribution and the form factor $P(q, R_s)$ is

$$P(q, R_s) = \frac{9}{q^6 R_s^6} (\sin(qR_s) - qR_s \cos(qR_s))^2. \quad (2)$$

In this discussion, the number distribution is chosen as a Gaussian distribution

$$G(R_s; \langle R_s \rangle, \sigma) = \frac{1}{\sigma\sqrt{2\pi}} \exp\left(-\frac{1}{2} \left(\frac{R_s - \langle R_s \rangle}{\sigma}\right)^2\right),$$

where $\langle R_s \rangle$ is the mean static radius and σ is the standard deviation relative to the mean static radius.

From the Stokes-Einstein relation

$$D = \frac{k_B T}{6\pi\eta_0 R_h},$$

where η_0 , k_B , T and R_h are the viscosity of the solvent, Boltzmann's constant, absolute temperature and hydrodynamic radius of a particle, respectively, the hydrodynamic radius can be obtained.

For simplicity, we assume that the relationship between the static and hydrodynamic radii is given by

$$R_h = aR_s, \quad (3)$$

where a is a constant. With the function between the normalized time auto-correlation function of the scattered light intensity $g^{(2)}(\tau)$ and the normalized time auto-correlation function of the electric field of the scattered light $g^{(1)}(\tau)$ [1]

$$g^{(2)}(\tau) = 1 + \beta \left(g^{(1)}\right)^2, \quad (4)$$

the relationship between SLS and DLS is built and the values of the normalized time auto-correlation function of the scattered light intensity $g^{(2)}(\tau)$ can be expected.

In this paper, the calculated and experimental values of $g^{(2)}(\tau)$ for two samples were compared. One is the polystyrene latex sample with the normalized size information: the mean radius is 33.5 nm and the standard deviation is 2.5 nm provided by the supplier, from Interfacial Dynamics Corporation (Portland, Oregon). The sample was diluted for light scattering to weight factor of 1.02×10^{-5} with fresh de-ionized water from a Milli-Q plus water system (Millipore, Bedford, with a 0.2 μm filter). The other is the poly(*N*-isopropylacrylamide) (PNIPAM) microgel sample with the molar ratio 1% of crosslinker *N,N'*-methylenebisacrylamide over *N*-isopropylacrylamide. The PNIPAM microgel sample was diluted to 8.56×10^{-6} . The size information was obtained fitting the SLS data. At a temperature of 302.33 K, the mean static radius is 254.3 ± 0.1 nm, the standard deviation is 21.5 ± 0.3 nm and χ^2 is 2.15 [2].

If the constant a for the polystyrene latex sample is assumed to be 1.1 and the size information provided by the supplier is thought to be consistent with that obtained from SLS, all the experimental and calculated values of $g^{(2)}(\tau)$ at a temperature of 298.45 K and the scattering angles 30° , 60° , 90° , 120° and 150° are shown in Fig. 1.a. When the constant a for the PNIPAM sample is assumed to be 1.21, all the experimental and calculated values at the scattering angles 30° , 50° and 70° are shown in Fig. 1.b. Figure 1 shows that the calculated values are consistent with the experimental data very well.

If the expected values were calculated using Barger's equation [3], all the experimental and calculated values of $g^{(2)}(\tau)$ for the polystyrene latex sample at the scattering angles 30° , 60° , 90° , 120° and 150° are shown in Fig. 2.a; all the experimental and calculated values for the PNIPAM sample at the scattering angles 30° , 50° and 70° are shown in Fig. 2.b. Figure 2 shows that the expected values have large differences with the experimental data.

Traditionally the size information is obtained from DLS. The standard method is the cumulant or the inverse Laplace transform. For the five experimental data of $g^{(2)}(\tau)$ measured under the same conditions as the SLS data, their corresponding fit results of $g^{(2)}(\tau)$ using the first cumulant and first two cumulant [4, 5] respectively for the PNIPAM microgel sample at a temperature of 302.33 K and a scattering angle of 30° are listed in Table 1.

	$\langle\Gamma\rangle_{first}$	χ^2	$\langle\Gamma\rangle_{two}$	μ_2	χ^2
1	79.5 ± 0.1	0.07	79.9 ± 0.3	28.20 ± 15.99	0.04
2	79.0 ± 0.1	0.33	80.4 ± 0.3	90.10 ± 17.11	0.04
3	79.7 ± 0.1	0.11	80.3 ± 0.3	39.17 ± 16.19	0.05
4	79.4 ± 0.1	0.07	79.7 ± 0.3	20.93 ± 15.92	0.06
5	78.7 ± 0.1	0.53	80.4 ± 0.3	112.75 ± 17.26	0.08

Table.1 The fit results for the PNIPAM sample at a temperature of 302.33 K and a scattering angle of 30° .

From the fit results, the values of the mean decay constant $\langle\Gamma\rangle$ show an independence on the measurements, but the results of μ_2 have a strong dependence on the measurements. The values of μ_2 are often negative. It's a contradiction with its definition. In order to discuss this problem conveniently, the simulated data are used.

The simulated data were produced using the size information: the mean static radius is 260 nm and the standard deviation is 26 nm. the temperature T was set to 302.33K, the viscosity η_0 of the solvent was 0.8132 mPa·S, the scattering angle was 30° and the constant a was chosen as 1.2. When the data of $(g^{(2)}(\tau) - 1) / \beta$ were obtained, the 1% statistical noises were added and the random errors were set 3%. Five simulated data were produced respectively. The fit results for the five simulated data using the first cumulant and first two cumulant respectively are shown in Table 2.

	$\langle\Gamma\rangle_{first}$	χ^2	$\langle\Gamma\rangle_{two}$	μ_2	χ^2
1	79.27 ± 0.01	11.98	79.90 ± 0.02	22.0 ± 0.6	7.75
2	78.50 ± 0.01	4.56	78.98 ± 0.03	9.8 ± 0.6	3.83
3	78.35 ± 0.01	5.67	79.43 ± 0.06	20.6 ± 1.2	4.66
4	78.33 ± 0.01	25.40	78.25 ± 0.02	-1.7 ± 0.4	25.44
5	78.596 ± 0.004	15.75	78.79 ± 0.02	4.9 ± 0.5	15.55

Table 2 The fit results for the simulated data with the standard deviation 26 nm.

From the fit results of the simulated data that are shown in Table 2, the situation is the same as the experimental data, the values of the mean decay constant $\langle\Gamma\rangle$ show an independence on the different noises and errors, and the results of μ_2 have a strong dependence on them. The values of μ_2 can be negative. As we have discussed, a truncated Gaussian distribution can give better results for the SLS data of the PNIPAM sample at a temperature of 302.33 K [2], so the five simulated data were produced respectively again with the truncated Gaussian distribution that the range of integral is 221 to 299 nm. The fit results for this five simulated data using the first cumulant and first two cumulant respectively are shown in Table 3. The values of the quantity μ_2 still have large differences for different simulated data and are often negative.

	$\langle\Gamma\rangle_{first}$	χ^2	$\langle\Gamma\rangle_{two}$	μ_2	χ^2
1	79.996 ± 0.002	10.96	79.73 ± 0.02	-5.4 ± 0.4	10.36
2	79.83 ± 0.01	20.57	79.79 ± 0.05	-0.95 ± 1.24	20.63
3	80.091 ± 0.004	5.30	80.69 ± 0.04	12.8 ± 0.8	4.61
4	79.926 ± 0.009	3.97	80.14 ± 0.03	4.3 ± 0.6	3.84
5	79.985 ± 0.005	9.00	80.48 ± 0.02	9.4 ± 0.3	5.51

Table 3 The fit results for the simulated data with the truncated distribution.

Comparing the fit results using the first cumulant with the values using the first two cumulant for the experimental and simulated data, the values of the mean decay constant can be thought to be equal. In order to avoid the contradiction that the values of μ_2 are often negative, the apparent hydrodynamic radius $R_{h,app}$ is obtained using the first cumulant. Meanwhile, from the analysis of cumulant, the apparent hydrodynamic radius is obtained from the average of the term $\exp(-q^2 D\tau)$ in distribution $G(R_s)$ with the weight $R_s^6 P(q, R_s)$. In order to explore the effects of the distribution, the simulated data were produced as the above simulated data with the same mean static radius 260 nm and the different standard deviations 13, 39 and 52 nm respectively. The constant a is still chosen 1.2. From this assumption, the mean hydrodynamic radius is 312 nm. The fit results for different standard deviations are listed in Table 4.

$\sigma/\langle R_s \rangle$	$R_{h,app} (nm)$
5%	315.7 ± 0.9
10%	$325. \pm 2.$
15%	339.4 ± 0.9
20%	$356. \pm 1.$

Table 4 The apparent hydrodynamic radii $R_{h,app}$ of the simulated data produced using the same mean static radius and different standard deviations.

From the results of apparent hydrodynamic radius, the values are obviously influenced by the values of standard deviation. As shown in Eq. 1, the quantity $\exp(-q^2 D \tau)$ is determined by the hydrodynamic characteristics of particles while $R_s^6 P(q, R_s)$ is determined by the optical features of particles. As a result, $g^{(2)}(\tau)$ is determined by both the optical and hydrodynamic characteristics of particles. When the cumulant method is used, the apparent hydrodynamic radius $R_{h,app}$ obtained from the normalized time auto-correlation function of the scattered light intensity $g^{(2)}(\tau)$ is a composite size. If the simple size information need to be obtained from $g^{(2)}(\tau)$, the relationship between the optical and hydrodynamic quantities of particles must be considered. The accurate relationship between the static and hydrodynamic radii can be further explored.

From above discussion, three different particle sizes can be obtained from the light scattering techniques. The static radius is determined by the optical characteristics, the hydrodynamic radius is obtained from the hydrodynamic features and the apparent hydrodynamic radius is determined by both the optical and hydrodynamic characteristics of particles. The function between the SLS and DLS can be built if the relationship between the optical and hydrodynamic quantities of particles can be understood.

Fig. 1 The expected and experimental values of the normalized time auto-correlation function of the scattered light intensity $g^{(2)}(\tau)$. Figures 1.a and 1.b show the results of the polystyrene latex and PNIPAM samples respectively. The symbols show the experimental data and the line shows the calculated values with the simple assumption $R_h = aR_s$.

Fig. 2. The expected and experimental values of the normalized time auto-correlation function of the scattered light intensity $g^{(2)}(\tau)$. Figures 2.a and 2.b show the results of the polystyrene latex and PNIPAM samples respectively. The symbols show the experimental data and the line shows the calculated values with the simple assumption $R_h = R_s$.

[1] P. N. Pusey in Neutrons, X-rays and Light: Scattering Methods Applied to Soft Condensed Matter, edited by P. Lindner and Th. Zemb, Elsevier Science B.V., Amsterdam, The Netherlands, 2002.

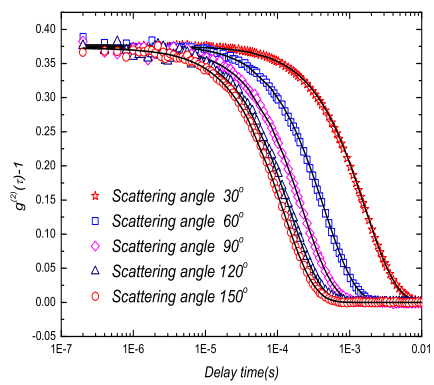
[2] Y. Sun, Unpublished (please see my second paper)

[3] C. B. Barger, J. Chem. Phys. 1974, 61, 2134.

[4] B. J. Berne and R. Pecora, Dynamic Light Scattering, Robert E. Krieger Publishing Company, Malabar, Florida, 1990.

[5] J. C. Brown, P. N. Pusey, R. Dietz, J. Chem. Phys. 1975, 62, 1136.

1). a



1). b

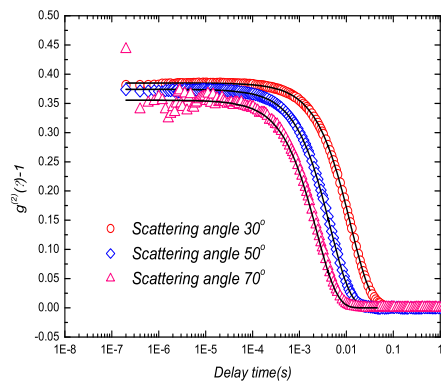
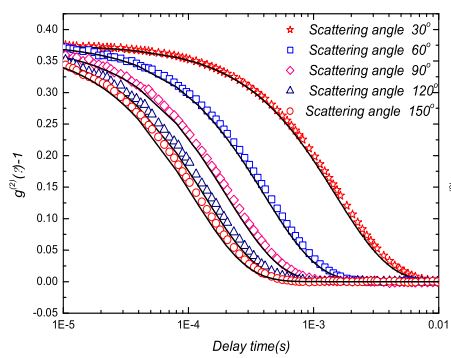


Fig. 1

2). a



2). b

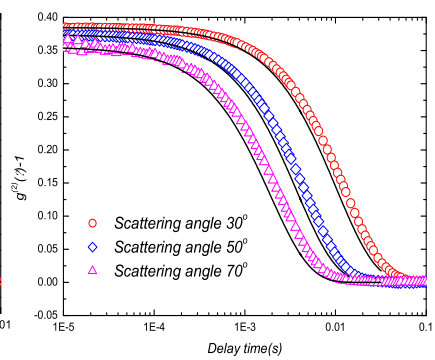


Fig. 2